PCCP

Cite this: *Phys. Chem. Chem. Phys.*, 2012, **14**, 13409–13414

www.rsc.org/pccp

PAPER

Theoretical studies on the isomerization mechanism of the *ortho*-green fluorescent protein chromophore†

Yue-Jie Ai,[ab] Rong-Zhen Liao,[c] Wei-Hai Fang*[b] and Yi Luo*[ad]

Received 19th April 2012, Accepted 10th August 2012
DOI: 10.1039/c2cp41959a

We present a systematic theoretical investigation on the overall ground state and excited-state isomerization reaction mechanism of *ortho*-green fluorescent protein chromophore (*o*-HBDI) using the density functional theory and the multireference methods. The calculated results and subsequent analysis suggest the possible isomerization mechanism for *o*-HBDI. By comparison with experimental observation and detailed analysis, it is concluded that as initiated by the excited-state intramolecular proton transfer reaction, the conical intersection between the ground state and the excited state along the C4–C5 single-bond rotational coordinate is responsible for the rapid deactivation of *o*-HBDI.

Introduction

The fascinating applications of the green fluorescent protein (GFP) in bio-imaging technology have inspired numerous experimental and theoretical studies.[1–3] As an analogue of the native GFP core (4-(4-hydroxybenzylidene)-1, 2-dimethyl-1*H*-imidazol-5(4*H*)-one, labelled as *p*-HBDI in Fig. 1), *o*-HBDI now gains much attention because of its special photochemical properties.[4–7] Several important differences have been observed between the *p*-HBDI and *o*-HBDI. The most important is that the *o*-HBDI possesses a seven-membered-ring intramolecular hydrogen bond, which thus provides an ideal model for mimicking an intrinsic excited state proton transfer reaction that dominates the photophysics of *wild type* GFP with the assistance of water molecules and residues in the active site.[8] Chen *et al.* first reported that there was a strong red-shifted emission spectrum at ~605 nm of *o*-HBDI in nonpolar solvents compared to the protein free *p*-HBDI, in which the excited-state proton transfer (ESPT) is prohibited and an extremely weak emission is observed.[4] The excited-state intramolecular proton transfer (ESIPT) was assigned between the *o*-OH and N atom of the imidazolinone ring (see structure "E" in Fig. 1).[5] In addition, due to structural change of the chromophore core, the excited-state relaxation dynamics was proposed to be different. For *p*-HBDI, it has been widely proposed that the rapid deactivation of *p*-HBDI is mainly governed by an efficient conical intersection between the ground and excited states induced by conformational relaxation along the *cis–trans*-isomerization.[3,9–13] While for *o*-HBDI, based on various ultrafast spectroscopic techniques, a proton transfer cycle was suggested, composed of "ESIPT → *cis–trans* isomerization → deprotonation → reverse ground-state protonation".[5] The *cis–trans* isomerization yield was estimated to be less than 5% and more than 95% of the excited state *o*-HBDI decay to the ground state. In another aspect, the rigid intramolecular hydrogen-bonding confines the rotation of the exocyclic C=C bond and results in controversial isomerization pathways, namely one-bond-flip (*o*-HBDI) *versus* the hula-twist (*p*-HBDI) mechanism.[5,14,15]

Since the intrinsic structural variation gives unique photochemical properties of *o*-HBDI in contrast to *p*-HBDI, a detailed study of the molecular/electronic structure is the first step for understanding the photophysical and photochemical properties of *o*-HBDI. Many efforts based on quantum chemical calculations and dynamical simulations have been devoted to the photophysics and photochemistry of *p*-HBDI in vacuum, solution and proteins.[3,12,16–18] In contrast, much less theoretical focus has been paid on *o*-HBDI. Very recently, Thiel and coworkers have investigated the absorption and emission spectra by quantum mechanical calculations at various levels, as well as OM2/MRCI nonadiabatic surface hopping simulations.[19] They found that the ultrafast excited-state intramolecular proton transfer, followed by the approach of a conical interaction, is responsible for the decay of the excited state *o*-HBDI. However, the full isomerization cycles in both the ground state and the excited state have not been studied, and the solvent effects were not considered that may affect the

[a] *Division of Theoretical Chemistry & Biology, School of Biotechnology, Royal Institute of Technology, S-106 91, Stockholm, Sweden. E-mail: luo@kth.se*
[b] *College of Chemistry, Beijing Normal University, Beijing 100875, China*
[c] *Max-Planck-Institut für Kohlenforschung, Kaiser-Wilhelm-Platz 1, D-45470, Mülheim an der Ruhr, Germany*
[d] *Hefei National Laboratory for Physical Sciences at the Microscale, Department of Chemical Physics, University of Science and Technology of China, Hefei, Anhui 230026, China*

† Electronic supplementary information (ESI) available: The detailed geometrical parameters for tautomers of structure D, the transition orbitals for excited state, calculated vertical excitation energies and oscillator strengths. See DOI: 10.1039/c2cp41959a

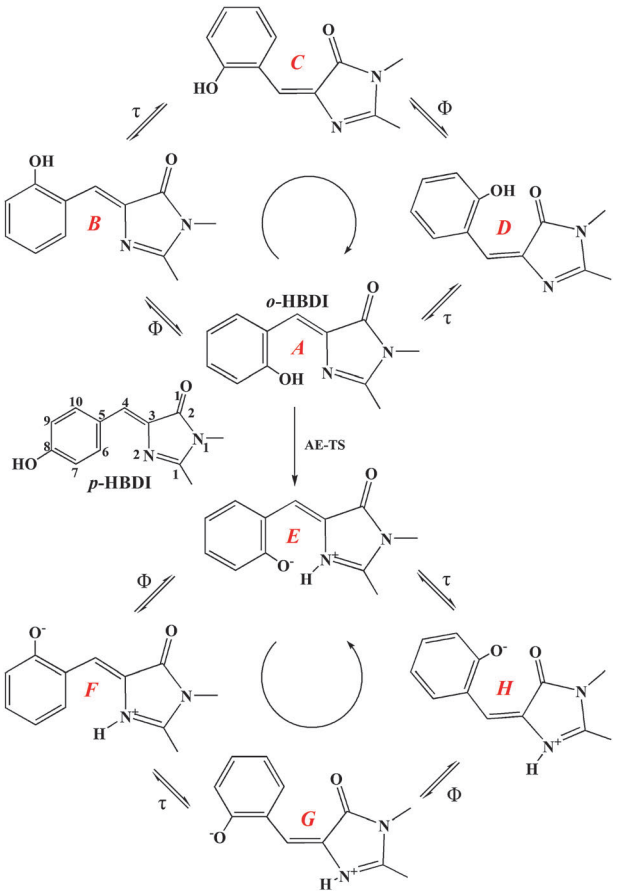

Fig. 1 Schematic structures of *p*-HBDI and *o*-HBDI, and possible isomerizations between different tautomers of *o*-HBDI.

vibrational activity and photodynamics of the chromophore.[12] In view of these perspectives, we used the density functional theory (DFT), complete active-space self-consistent field (CASSCF) and complete active space with second-order perturbation theory (CASPT2) methods to study the excited-state relaxation path and isomerization mechanism of the free *o*-HBDI chromophore *in vacuo* and solution. We show a clear mechanistic picture of the isomerization process and also the fluorescence decay channel of *o*-HBDI.

Computational details

All stationary points (including transition states) of the ground states were optimized at the DFT level with the B3LYP hybrid functional.[20] The minima and transition states were verified by calculating harmonic vibrational frequencies. Since the complete π-system for *o*-HBDI is too large and expensive for CASSCF calculations, the excited state geometries were optimized using the CASSCF method with a reduced active space of 12 electrons in 11 π-orbitals [denoted as CAS(12,11)], which is widely used in former theoretical calculations.[11,12] In order to obtain more reliable energies, single-point calculations were performed at the multiconfigurational second-order perturbation theory (CASPT2)[21] level at the optimized CASSCF geometries. The vertical excitation and emission energies and their oscillator strengths were calculated by the time-dependent density functional theory (TDDFT) method. To consider the solvent effect, the polarizable continuum model (PCM)[22–24] for the acetonitrile solvent is applied. A standard 6-31G(d) basis set was used throughout the calculations.[25,26] All the calculations were carried out by using the Gaussian 09 package[27] and the MOLCAS 6.4 quantum chemistry software.[28]

Results and discussions

Isomerization in the ground state

In the present work, two torsional angles *Φ* (C10C5C4C3) and *τ*(C5C4C3C2) as defined in ref. 11 are used to describe the rotation of the C5–C4 and C3═C4 bonds. With the rotation around the two ring-bridging C–C bonds, the isomerization of *o*-HBDI can produce several tautomers. As shown in Fig. 1, eight possible chemical tautomers of the *o*-HBDI molecule were studied. The ground-state optimized structural parameters for the energy minima and transition states are presented in Fig. 2 and Fig. 3, respectively, and the relative energies are listed in Table 1.

Structure A of the *o*-HBDI molecule is the most stable one among all the tautomers because of its strong hydrogen bond (1.65 Å) between C6–OH and the N2 atom, see Fig. 2. This intramolecular hydrogen-bonding forms a seven-membered ring and keeps the structure A to be planar. Starting from structure A, the C4–C5 single-bond rotation around angle *Φ*

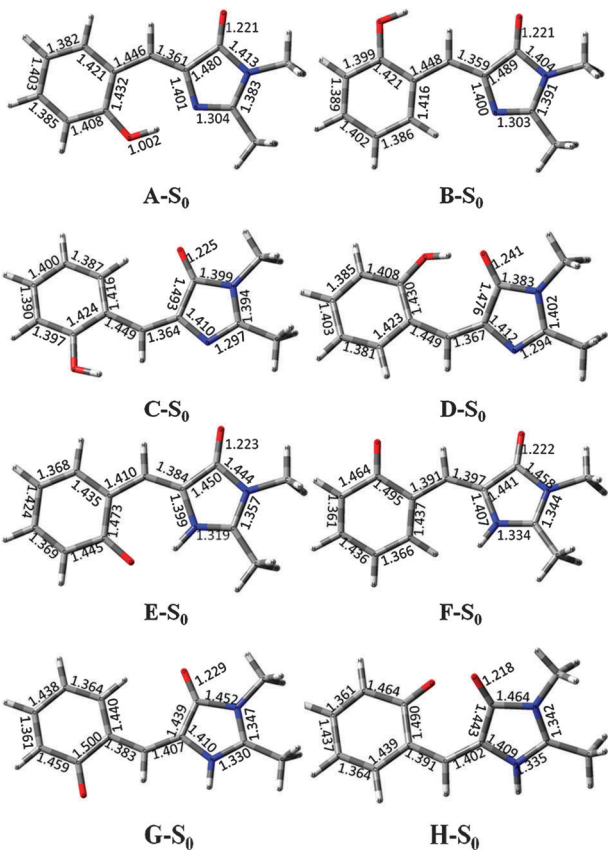

Fig. 2 Optimized structural parameters of tautomers for *o*-HBDI in the ground state predicted at the B3LYP/6-31G(d) level. The geometrical parameters are given in Å.

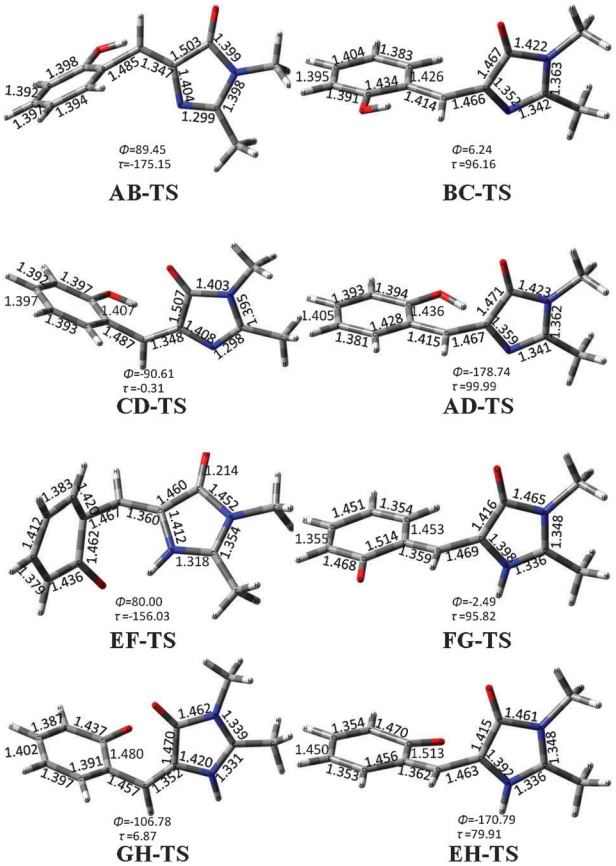

Fig. 3 Optimized structural parameters for transition states in the ground state at the B3LYP/6-31G(d) level. The geometrical parameters are given in Å and degrees.

Table 1 Relative energies for the ground state *o*-HBDI in vacuum and acetonitrile solution

Structure	B3LYP/6-31G(d) kcal mol^{-1} vacuum (PCM)	Structure	B3LYP/6-31G(d) kcal mol^{-1} vacuum (PCM)
A	0.00 (0.00)	AB-TS	15.04 (14.03)
B	9.53 (8.84)	BC-TS	47.81
C	12.71 (12.14)	CD-TS	16.53 (15.48)
D	7.13 (7.20)	AD-TS	47.48
E	10.32 (5.47)	EF-TS	49.64 (36.40)
F	28.96 (16.88)	FG-TS	46.68 (40.03)
G	27.21 (16.32)	GH-TS	64.04 (39.56)
H	36.49 (23.32)	EH-TS	49.69 (43.43)

leads to the planar structure B that is 9.53 kcal mol^{-1} higher than A. We optimized the transition state between these two isomers, which is labeled as AB-TS in Fig. 3. The torsional angle Φ is 89° in AB-TS and the isomeric barrier from A to B is about 15 kcal mol^{-1}. These results suggest that structure B cannot be observed at room temperature, and B will decay to A rapidly. Subsequent rotation from structure B to C has a much higher reaction barrier (38.28 kcal mol^{-1}) with the angle τ of 96°. The same situation holds for the rotation between A and D with the barrier of around 47 kcal mol^{-1}. It is obvious that one double bond (C3═C4) has to be broken during these two isomerization processes. For example, the C3═C4 double bond is 1.359 Å at B and elongated to 1.466 Å in BC-TS. As shown in Fig. 3, the torsional angle of structure CD-TS and AD-TS is 90° and 100°, respectively. Structures C and D are nonplanar with a relative energy of 12.71 and 7.13 kcal mol^{-1}, respectively. The isomeric barrier between C and D with angle Φ is only 3.82 kcal mol^{-1}. In contrast to concerted hula-twist type of motion for *p*-HBDI,[14,15] the present results suggest that the possible isomerization of *o*-HBDI in the ground state follows the C4–C5 single-bond rotation mechanism around angle Φ to access structure B.

It is worth mentioning that structure D also forms a seven-membered ring with intramolecular hydrogen-bonding between C6–OH and the O1 atom, thus hydrogen transfer may take place from C6–OH to O1 or C3, called (1–7) or (1–5) hydrogen transfer, respectively. However, the former is much easier than the latter due to its lower energy barrier (8 kcal mol^{-1} *vs.* 36 kcal mol^{-1}), see ESI† for details.

The intramolecular proton transfer between C6–OH and N2 results in structure E, which is unstable in the ground state and has the energy of 10.32 kcal mol^{-1}, see Fig. S2 (ESI†). Similar to the upper cycle in Fig. 1, the isomerization of E is presented in the lower cycle. Compared to structure A, on the one hand, the tautomers of structure E (F, G, H) have high energies, so do the transition states between them. One can see from Fig. 2, instead of the alternating single and double bond property, the linking carbon-bridge is much more delocalized in these tautomers. On the other hand, different from the isomerization mechanism of structure A, the transition states along angle τ, like FG-TS and EH-TS, have lower reaction barriers than EF-TS and GH-TS (along angle Φ). However, in the ground state, due to the high reaction barrier, it is impossible for the conversion of E isomer into either F or H.

Based on the above results, we then optimized the structures with the inclusion of solvent effect by the PCM model. The calculated relative energies are presented in Table 1, and one may see structural information in ESI.† The solvent interactions stabilized both the tautomers and the transition states with lower relative energies, as shown in Table 1. Especially for the lower cycle in Fig. 1, due to the solvent effects, there is a significant drop in the energy of tautomer E, F, G, H and their transition states. However, the rotational barrier along angle τ is still much higher compared to the C4–C5 single-bond rotation mechanism, and this is may be the reason for the convergence problems in BC-TS and AD-TS.

Isomerization in the excited-state and excited-state relaxation pathway

Experimentally, the steady-state absorption peak of *o*-HBDI in acetonitrile is around 380 nm.[5] We calculated the vertical excitation energy of *o*-HBDI in the acetonitrile solution by the TDDFT-PCM method. As shown in Table 2, the calculated value, 3.39 eV (365.53 nm, f = 0.3851), is in good agreement with the experiment. Upon excitation by light with 385 nm in wavelength, *o*-HBDI is promoted to the first excited state S_1. Hsieh *et al.* proposed that ESIPT takes place immediately (<25fs) upon excitation and results in a proton-transfer tautomer with emission at 602 nm.[5] In their TDDFT optimization, they failed to locate the minimum of the excited state of *o*-HBDI and thus deduced that this ESIPT is barrierless along the

Table 2 Calculated vertical excitation and emission energies at the TDDFT/PCM//B3LYP/6-31G(d) level in acetonitrile

Absorption structure	TDDFT/PCM//B3LYP/6-31G(d) (eV)	*f*
o-HBDI (A)	3.39	0.3851
H	2.56	0.2540
H(anion)	2.63	0.2607
F	2.63	0.5763
F(anion)	2.73	0.5790
Emission structure	**TDDFT/PCM//B3LYP/6-31G(d) (eV)**	***f***
o-HBDI(A*)	2.95	0.2994
o-HBDI-ESIPT(E*)	2.25	0.2008

reaction coordinate.[4] The former CC2/TZVP S_1 geometry optimization starting from the Franck–Condon (FC) S_0 geometry (A) ends up at the proton-transfer S_1 minimum (E*), indicating a barrierless ESIPT process.[19] Our TDDFT optimization from the FC S_0 geometry of *o*-HBDI also gets its ESIPT tautomer (E*) with an energy of 2.14 eV above the ground state of E.

However, in our CASSCF calculations, we indeed found the minimum structure of the S_1 state of *o*-HBDI which is A-S_1 in Fig. 4. The excitation mainly locates in the phenyl ring, linking bridge and partly the imidazolinone ring; and the relative energy is 75.68 kcal mol^{-1} by a CASPT2 single point energy calculation, with the inclusion of solvent effect through the PCM method. The involved transition orbitals are visualized in Fig. S3 (ESI†). The CASSCF calculated S_0 and S_1 permanent dipole moment at the FC point is 3.69 and 6.71D, respectively, indicating the partial charge-transfer character for the S_1 state, as proposed by a previous theoretical study.[19] The optimized structure of the corresponding ESIPT tautomer (E-S_1) is also shown in Fig. 4. It is 12.18 kcal mol^{-1} more stable than A-S_1 in solution. We attempted to locate the transition state along the proton transfer coordinate, which is A-E-TS-S_1 in Fig. 4, with the O–H distance of 1.128 Å and a corresponding imaginary frequency of 1107.9i cm^{-1}. It is only about 3 kcal mol^{-1} above the minimum A-S_1 at the CASSCF/6-31G(d) level in vacuum, see Fig. S4 (ESI†). The CASPT2 single-point corrected energy of A-E-TS-S_1 is 69.91 kcal mol^{-1} in solution, *i.e.*, almost 6 kcal mol^{-1} below the corresponding value for A-S_1 (see Table 3).

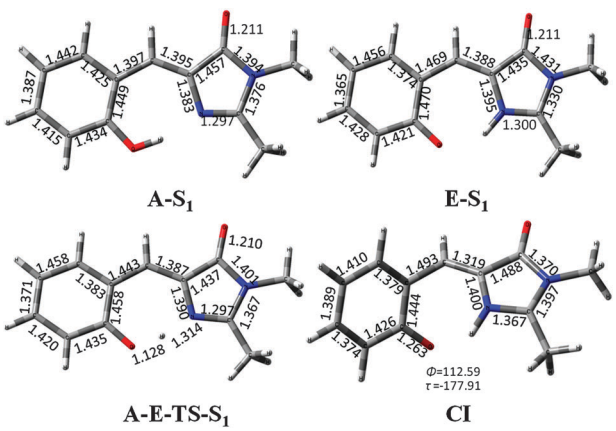

Fig. 4 Optimized structural parameters for the minimum, transition states and conical intersection in the excited state predicted at the CASSCF/6-31G(d) level. Bond lengths and dihedrals are given in Å and degrees, respectively.

Table 3 CASPT2/PCM//CASSCF single point energies for the *o*-HBDI in acetonitrile solution

Structure	CASPT2/PCM// CASSCF kcal mol^{-1} (eV)
A-S_1(A*)	75.68 (3.28)
E-S_1(E*)	63.50 (2.75)
A-E-TS-S_1	69.91 (3.03)
CI	57.25 (2.48)

On the basis of these more reliable CASPT2 results, we conclude that the ESIPT in the excited state of *o*-HBDI can be considered to be a quasi-barrierless process, consistent with the experimental finding that is completed with 25 fs[5] and also the former CC2/TZVP results.[19]

Previous experiment has also resolved a steady-state emission peak of *o*-HBDI in acetonitrile at 602 nm,[5] which was tentatively assigned to the emission from the state E*. Our computed emission energies and oscillator strengths of all relevant states in acetonitrile at the PCM//TDDFT//B3LYP/6-31G(d) level are listed in Table 2. From the computed results, it could be suggested that the ESIPT tautomer of *o*-HBDI should be a possible emitter since its calculated emission energy (2.25 eV) agrees well with the experiment (2.06 eV), implying the nature of the emission to be the E-S_1 state, whereas the A-S_1 has very high energy (2.95 eV). That is to say, upon electronic excitation, the ultrafast ESIPT process takes place and the excited *o*-HBDI (A*) turns into its ESIPT tautomer (E*). The experimental hypothesis is thus verified and complemented by our theoretical calculations.

Initiated by the excited-state intramolecular proton transfer reaction, the proton transfer isomer may undergo isomerization in the excited state. For the sake of computational efficiency, we first did the TDDFT excited-state geometry optimizations with fixed values of Φ angles along the reaction coordinate and the scanned energy profile is represented in Fig. 5. One can see that along the rotation of Φ angle, the energy of the excited state S_1 decreases slowly, while that of the ground state S_0 increases sharply. At the twisted

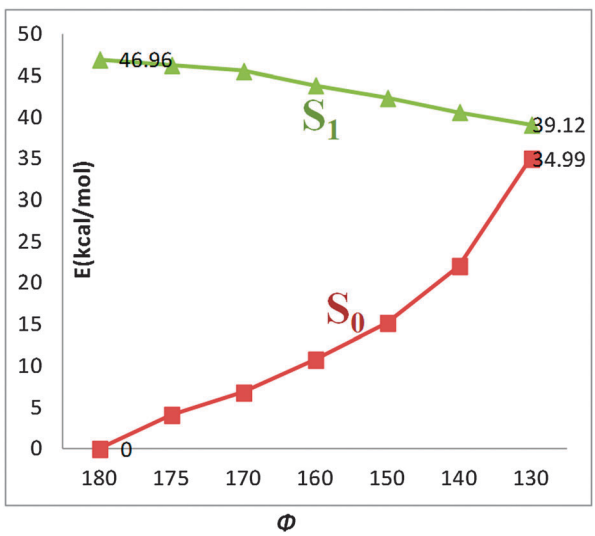

Fig. 5 TDDFT optimized energy profile for the S_0 and S_1 states along the torsional angle Φ.

geometry of 130°, both the ground and excited states potential energy surfaces approach toward each other and the energy difference is only 4.13 kcal mol^{-1} at the TDDFT/B3LYP/6-31G(d) level. Base on above calculations, we speculate there should be a conical intersection between the ground and excited states at this region and it may give rise to a rapid internal conversion process similar to the exited-state relaxation of free *p*-HBDI.[9–11] Further support was then given by the CASSCF calculations. Since the direct optimization of conical intersection with large active space is time-consuming and beyond the limited computation resources, we used a relatively small active space CAS(8,7) to optimize the conical intersection (CI). The optimized structure is shown in Fig. 4. The Φ angle is about 112° in CI and the relative energy is 49.27 kcal mol^{-1} by single-point calculation at the CASPT2//CASSCF(12,11)/6-31G(d) level. We provide the CASPT2 single-point energies for the S_0 and S_1 states at the CI point for both small CAS(8,7) and the standard CAS(12,11) space in ESI.† The S_0–S_1 energy gap at the CI point indicates that the conical intersection is only 5.6 and 5.8 kcal mol^{-1} at the CASPT2//CASSCF(12,11) level in vacuum and solution, respectively.

It is worth mentioning that compared to the gas phase, in solution environment, the geometrical or charge changes induced by solvent may drive an alternative relaxation channel that is different from that preferentially followed in the gas phase. Altoe *et al.*[12] proposed that in contrast with the favoured single CC bond rotation mechanism in the gas phase, the channel upon rotation around the exocyclic CC double bond is the dominant radiationless decay pathway for the HBDI chromophore in solution.

Here, we also investigated the excited-state photoisomerization along the rotation of τ angle. The excited-state energy increases along with the rotational coordinate and is highly above the ground state, see Fig. S5 in ESI.† If we compared with *p*-HBDI and *o*-HBDI, because of the strong intra-molecular hydrogen bonding between C6–OH and N2 atoms, the torsional coordinate along the τ angle is significantly hindered, leading to relatively high rotational barriers.

To summarize, we draw the possible isomerization mechanism in Fig. 6. After the ESIPT process in the first singlet excited state, through the C4–C5 single-bond rotation around angle Φ, the potential energy surface of E* finally meets the ground state potential energy surface at the CI point and then the following rapid internal conversion process produces the ground state product E. Since the ground state hydrogen transfer from E to the tautomer A is barrierless finally the whole excited-state deactivation ended in A. This is in agreement with experimentally >95% recovery of the stimulated emission at the early 130 ps time regime.[5] However, there was still a small portion, about 5%, of the long-lived *trans*-tautomer detected. Hsieh *et al.* proposed this ground-state *trans*-tautomer to be structure H and which is then deprotonated, forming an anion species (H-anion) in a polar solvent.[5] In our calculation, the possibility of formation of the H product is low because of the relatively high barrier (EH-TS) in the ground state, see Table 1. On the other hand, tautomer E may also overcome transition states EF-TS to form product F in the ground state. However, the reaction barrier is very high in the ground state. However, the isomerization from E to F in the excited state is

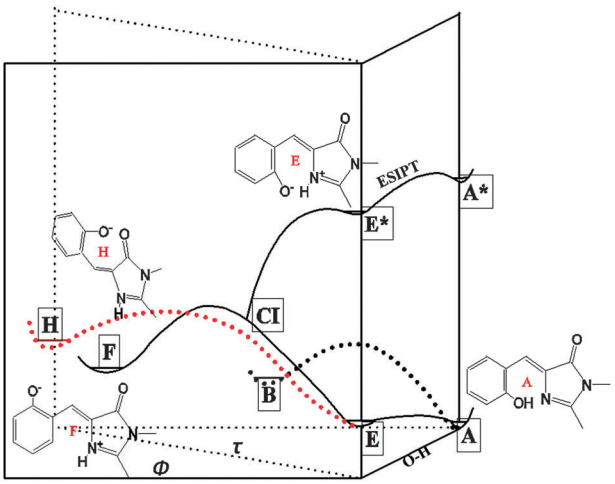

Fig. 6 Isomerization mechanism and excited-state deactivation pathway for *o*-HBDI along the relaxation coordinates.

along the rotational coordinate of Φ angle which is in consistent with the CI point. The structure of EF-TS is similar to the CI point with several different torsional parameters. If we compared the energies computed at the same level, the EF-TS (49.64 kcal mol^{-1}) is close to the CI point (around 40 kcal mol^{-1} at TDDFT/B3LYP/6-31G(d) level, see Fig. 5). Thus, we cannot rule out the possible excited-state deactivation channel *via* the CI point and subsequent ground-state isomerization along Φ angle, leading to tautomer F. The calculated vertical absorption energy of H and F and also their anion species are shown in Table 2. For other tautomers, see Table S1 (ESI†). From the computed absorption energies and oscillator strengths we exclude the H and F molecules from the possible absorption spectrum at 570 nm. The experimentally observed 570 nm absorption might come from the intermediate structure during the *cis–trans* isomerization. On the other hand, the anion forms of A, tautomer F and its anion forms could both be possible candidates responsible for the absorption at 490 nm.

Further, we give a comparison of the calculated results in this work and ref. 19. First, we considered both Φ and τ rotations in the ground state and also the excited state. Second, for the conical intersection point, in Cui *et al.*'s calculations, the conical intersection is said to be geometrically close to E* and lies 5.5 kcal mol^{-1} above E*. In our work, the structure of CI is similar to that reported in ref. 19. However, the calculated PES along the reaction coordinate indicates that it is barrierless from E* to the CI point. This deviation may come from the symmetric restriction of S1-MIN in ref. 19. Third, in ref. 19, the observed 5% *trans* conformer is supposed to be produced by a ground-state isomerisation from A to B with a barrier of 15 kcal mol^{-1}. However, for tautomer B, our computed absorption energy (3.3084 eV, 374.76 nm) is totally deviated from the experimental observations (570 nm and 490 nm). In contrast, we proposed the possible population of *trans* conformer F which is driven by excited-state isomerization along angle Φ. The major concern in our present work is that we investigate the solvent effect on the deactivation channels of the *o*-HBDI in solution, which is not considered in ref. 19.

Conclusions

By means of the density functional theory (DFT) and multi-reference methods, we studied the ground-state and excited-state isomerization mechanism and the excited-state relaxation pathway of the *ortho*-green fluorescent protein chromophore (*o*-HBDI). The isomerization of *o*-HBDI mainly follows the C4–C5 single-bond rotation mechanism. By comparison with the experimental observations and detailed analysis, we present a hypothesis that can be accomplished in the following steps: upon the excitation of the 380 nm band, the *o*-HBDI is excited to its first singlet excited state A*, and an ultrafast excited-state intramolecular proton transfer reaction produces its ESIPT tautomer E*, the latter is assigned to an experimental emission peak at 602 nm. The subsequent conical intersection (CI) between the ground-state and the excited-state along the C4–C5 single-bond rotational coordinate is responsible for the rapid deactivation pathway of *o*-HBDI, while isomerization near the CI point leads to the product of F isomer in the S_0 state. The inclusion of the solvent effects is crucial to the isomerization process in both the ground and excited states.

Acknowledgements

This work was supported by Natural Science Foundation of China (20925311), the Göran Gustafsson Foundation for Research in Natural Sciences and Medicine. The Swedish National Infrastructure for Computing (SNIC) is acknowledged for computer time.

Notes and references

1 R. Y. Tsien, *Ann. Rev. Biochem.*, 1998, **67**, 509–544.
2 M. Zimmer, *Chem. Rev.*, 2002, **102**, 759–781.
3 S. R. Meech, *Chem. Soc. Rev.*, 2009, **38**, 2922–2934.
4 K. Y. Chen, Y. M. Cheng, C. H. Lai, C. C. Hsu, M. L. Ho, G. H. Lee and P. T. Chou, *J. Am. Chem. Soc.*, 2007, **129**, 4534–4535.
5 C. C. Hsieh, P. T. Chou, C. W. Shih, W. T. Chuang, M. W. Chung, J. Lee and T. Joo, *J. Am. Chem. Soc.*, 2011, **133**, 2932–2943.
6 K. C. Tang, M. J. Chang, T. Y. Lin, H. A. Pan, T. C. Fang, K. Y. Chen, W. Y. Hung, Y. H. Hsu and P. T. Chou, *J. Am. Chem. Soc.*, 2011, **133**, 17738.
7 W. T. Chuang, C. C. Hsieh, C. H. Lai, C. W. Shih, K. Y. Chen, W. Y. Hung, Y. H. Hsu and P. T. Chou, *J. Org. Chem.*, 2011, **76**, 8189–8202.
8 K. Brejc, T. K. Sixma, P. A. Kitts, S. R. Kain, R. Y. Tsien, M. Ormo and S. J. Remington, *Proc. Natl. Acad. Sci. U. S. A.*, 1997, **94**, 2306–2311.
9 S. S. Stavrov, K. M. Solntsev, L. M. Tolbert and D. Huppert, *J. Am. Chem. Soc.*, 2006, **128**, 1540–1546.
10 R. Gepshtein, D. Huppert and N. Agmon, *J. Phys. Chem. B*, 2006, **110**, 4434–4442.
11 M. E. Martin, F. Negri and M. Olivucci, *J. Am. Chem. Soc.*, 2004, **126**, 5452–5464.
12 P. Altoe, F. Bernardi, M. Garavelli, G. Orlandi and F. Negri, *J. Am. Chem. Soc.*, 2005, **127**, 3952–3963.
13 S. Olsen and S. C. Smith, *J. Am. Chem. Soc.*, 2008, **130**, 8677–8689.
14 W. Weber, V. Helms, J. A. McCammon and P. W. Langhoff, *Proc. Natl. Acad. Sci. U. S. Am.*, 1999, **96**, 6177–6182.
15 R. S. H. Liu, *Acc. Chem. Res.*, 2001, **34**, 555–562.
16 P. J. Tonge and S. R. Meech, *J. Photochem. Photobiol., A*, 2009, **205**, 1–11.
17 D. Mandal, T. Tahara and S. R. Meech, *J. Phys. Chem. B*, 2004, **108**, 1102–1108.
18 S. Olsen, K. Lamothe and T. J. Martinez, *J. Am. Chem. Soc.*, 2010, **132**, 1192–1193.
19 G. L. Cui, Z. G. Lan and W. Thiel, *J. Am. Chem. Soc.*, 2012, **134**, 1662.
20 A. D. Becke, *J. Chem. Phys.*, 1993, **98**, 5648.
21 K. Andersson, P.-Å. Malmqvist and B. O. Roos, *J. Chem. Phys.*, 1992, **96**, 1218.
22 M. Cossi and V. Barone, *J. Chem. Phys.*, 2001, **115**, 4708–4717.
23 M. Cossi, V. Barone and M. A. Robb, *J. Chem. Phys.*, 1999, **111**, 5295–5302.
24 M. Cossi, G. Scalmani, N. Rega and V. Barone, *J. Chem. Phys.*, 2002, **117**, 43–54.
25 M. M. Francl, W. J. Pietro, W. J. Hehre, J. S. Binkley, M. S. Gordon, D. J. DeFrees and J. A. Pople, *J. Chem. Phys.*, 1982, **77**, 3654–3665.
26 P. C. Hariharan and J. A. Pople, *Theor. Chim. Acta*, 1973, **28**, 213–222.
27 M. J. Frisch, G. W. Trucks, H. B. Schlegel, G. E. Scuseria, M. A. Robb, J. R. Cheeseman, G. Scalmani, V. Barone, B. Mennucci, G. A. Petersson, H. Nakatsuji, M. Caricato, X. Li, H. P. Hratchian, A. F. Izmaylov, J. Bloino, G. Zheng, J. L. Sonnenberg, M. Hada, M. Ehara, K. Toyota, R. Fukuda, J. Hasegawa, M. Ishida, T. Nakajima, Y. Honda, O. Kitao, H. Nakai, T. Vreven, J. A. Montgomery, Jr., J. E. Peralta, F. Ogliaro, M. Bearpark, J. J. Heyd, E. Brothers, K. N. Kudin, V. N. Staroverov, R. Kobayashi, J. Normand, K. Raghavachari, A. Rendell, J. C. Burant, S. S. Iyengar, J. Tomasi, M. Cossi, N. Rega, N. J. Millam, M. Klene, J. E. Knox, J. B. Cross, V. Bakken, C. Adamo, J. Jaramillo, R. Gomperts, R. E. Stratmann, O. Yazyev, A. J. Austin, R. Cammi, C. Pomelli, J. W. Ochterski, R. L. Martin, K. Morokuma, V. G. Zakrzewski, G. A. Voth, P. Salvador, J. J. Dannenberg, S. Dapprich, A. D. Daniels, Ö. Farkas, J. B> Foresman, J. V. Ortiz, J. Cioslowski and D. J. Fox, *Gaussian 09*, Gaussian, Inc., Wallingford, CT, 2009.
28 G. L. R. Karlström, P.-Å. Malmqvist, B. O. Roos, U. Ryde, V. Veryazov, P.-O. Widmark, M. Cossi, B. Schimmelpfennig, P. Neogrady and L. Seijo, *Comput. Mater. Sci.*, 2003, **28**, 222.